ESTABLISHMENT OF MATHEMATICAL MODEL FOR AN EXPERIMENTAL FULL-SCALE BUILDING WITH ACTIVE BRACING SYSTEM

Jong-Cheng WU[1], Chin-Hsiung LOH[2] And Jann N. YANG[3]

SUMMARY

Recently, the application of active control to seismic-excited buildings has attracted international attentions. To demonstrate the practical applicability of active control, we have conducted experimental tests using a full-scale three-story building equipped with active bracing systems on the shake table at the National Center for Research on Earthquake Engineering (NCREE), Taiwan. Experimental results indicate that the control-structure interaction (CSI) effect is significant. A state-space analytical model of this actively controlled building taking into account the CSI effect is established in this paper using a system identification technique based on the curve-fitting of transfer functions. To verify the accuracy of the analytical model for simulating the controlled response, five sets of Linear Quadratic Gaussian (LQG) controllers using acceleration feedbacks are designed and further experimental tests are conducted. It is demonstrated that the correlations between the simulation and experimental results are remarkable. The construction of an accurate analytical model is important for active control, and such an analytical model can be used for future benchmark studies of different control algorithms based on numerical simulations.

INTRODUCTION

Considerable research efforts have been made in the last two decades for the application of active control to civil engineering structures, including analytical studies or experimental verifications [e.g., Kobori (1998)]. Several well-developed algorithms in control engineering have been successfully introduced to active control of civil structures, such as optimal control [e.g., Yang (1975)], sliding mode control [e.g., Yang et al (1995, 1997), Wu et al (1998b)], H_2 [e.g., Spencer et al (1994)] and H_∞ [e.g., Wu et al (1998a, b)], just to name a few. The performances and applicabilities of these control methods to civil structures have been verified by numerical simulation results and/or experimental tests on the shake table using scaled models. Experimental verifications on the shake table using a full-scale model are particularly desirable because of the complexity involved in implementing active control systems. In the past, experimental tests on the shake table have been conducted using small scaled models equipped with active control devices and the results have been presented in the literature [e.g., Chung et al. (1989), Dyke et al. (1994a,b,c), Yang and Wu et al. (1996a, b), etc.]. Through experimental research, important experience has been gained toward the implementation of active control systems on full-scale structures.

Traditionally, the nominal system for active controller design is identified without considering the control-structure interaction (CSI) effect, i. e., the dynamics of the structure and the dynamics of control device are identified individually [Chung et al. (1989), Yang and Wu et al. (1996a, b)]. Then, a constant time delay is observed from the active device (actuator), and different time delay compensation techniques are used to improve the control performance [e. g., Chung et al (1995)]. The significance of CSI effect in actively controlled civil structures was first demonstrated by [Dyke et al. (1994c)] using a small scaled building model. It was shown that the transfer function of the actuator installed on the structural model contains more complex dynamics than just a constant time delay. By incorporating the CSI effect in the nominal system, the H_2 controllers using acceleration feedbacks are shown to be successful [Dyke et al. (1994a,b)]. However, the significance of CSI for full-scale structures is yet to be demonstrated experimentally.

[1] *Department of Civil Engineering,Tamkang University, Taipei, Taiwan, email: jcwu@bridge.ce.tku.edu.tw*
[2] *National Center for Research on Earthquake Engineering, Taipei, Taiwan,email: lohc@email.ncree.gov.tw*
[3] *Department of Civil and Environmental Engineering, University of California, Irvine, U.S.A., email: jnyang@uci.edu*

In this paper, we have conducted experimental tests using a full-scale three-story building equipped with active bracing systems on the shake table at the National Center for Research on Earthquake Engineering (NCREE), Taiwan. The objectives of this paper are : (1) to demonstrate the significance of CSI effect on this full-scale building based on the experimental results on the shake table, (2) to construct an analytical model incorporating the CSI effect using a system identification method based on the curve-fitting technique, and (3) to verify experimentally the accuracy of the analytical model for simulating the controlled response of the building using Linear Quadratic Gaussian (LQG) controllers based on acceleration feedbacks. It is demonstrated that the correlations between the simulation and experimental results are remarkable. This is the first attempt in the literature to demonstrate experimentally the CSI effect using a full-scale building and to provide an accurate analytical model of the building for future benchmark studies of different control algorithms.

EXPERIMENTAL SETUP

Fig. 1: 3-Story Full-Scale Building on Shake Table of NCREE, Taiwan

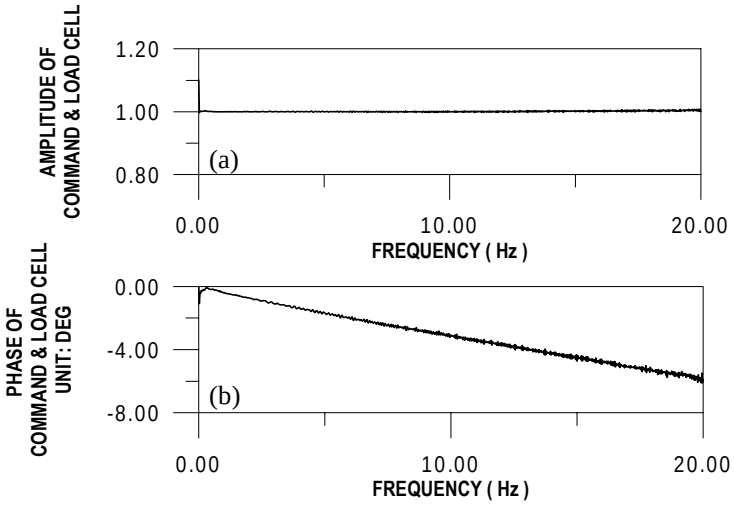

Fig. 2: Transfer Function of Hydraulic Actuator; (a) Amplitude, and (b) Phase Angle

A full-scale three-story building made of spatial steel rigid frame was constructed at the National Center for Research on Earthquake Engineering (NCREE) in Taiwan for experimental tests on the shake table, as shown in Fig. 1. The building has a rectangular shape with a floor area of 4.5 m by 3m in each floor and a total height of 9 m (3m for each story). Earthquake excitations were applied in the direction of weaker axis *x*, that is the axis along the length of 4.5 m as shown in Fig. 1. The dead loads are represented by three lumped masses of concrete blocks on the top of each floor. These masses are 1144.16 $\text{kgf}\cdot\text{s}^2/\text{m}$ for the first two floors and 1113.62 $\text{kgf}\cdot\text{s}^2/\text{m}$ for the top floor. An active bracing system consists of a highly stiffened steel tube connected in series with a hydraulic MTS dynamic actuator. The capacity of the hydraulic actuator is 2.5 ton force and the servo-controller is programmed to track a command signal of force (force control). The transfer function of the output/input relation of the hydraulic actuator was carefully tested before the installation of active bracing systems on the building, and the results are presented in Fig. 2. As shown in Fig. 2, the actuator performs quite well except the existence of a slight constant time delay (about 0.8 msec). Two of such an active bracing system were installed diagonally between the ground and first floor, one on each side of the building along the *x* direction. To prevent the undesirable motion in the transverse (*y*) direction, a few stiffeners were added to the bracing system to ensure the building motion in the x direction.

During experimental tests, eight response quantities of the building are recorded. These include (i) the relative displacements x_i (w.r.t. the ground) and absolute accelerations $\ddot{x}_{ai}$ of each floor which are measured by the LVDT sensors and accelerometers, respectively, (ii) the stroke x_f of actuator which is measured by the build-in LVDT probe inside the actuator, and (iii) the internal force f in the bracing which is measured by the load cell on the bracing. In what follows, these quantities are denoted by a vector $\mathbf{z} = [\, x_1, x_2, x_3, x_f, \ddot{x}_{1a}, \ddot{x}_{2a}, \ddot{x}_{3a}, f \,]^T$. Since the displacement sensors are not quite practical and are most expensive, the displacements are not considered herein as the measured quantities for feedback control. For the purpose of comparison, the shake table tests for the bare frame building and the building equipped with active

bracings (but zero command) are first conducted using the 1940 El Centro (100 seconds) and 1995 Kobe (60 seconds) earthquakes with a 0.1g PGA. The preliminary study shows that the three natural frequencies and damping ratios of the building itself are about 6.673, 21.783 and 37.506 rad/sec, and 0.81%, 0.25% and 0.34%, respectively, whereas the frequencies and damping ratios of the building with active bracing systems (zero command) are about 7.363, 22.933 and 37.966 rad/sec, and 1.38%, 2.46% and 1.32 %, respectively.

SYSTEM IDENTIFICATION

The control-structure interaction can be investigated by analyzing the output/input transfer function of the active bracing system in the building. By using a 0-30 Hz banded white noise signal for the actuator command, the transfer function is obtained by measuring the corresponding active bracing force as shown in Fig. 3. The result shown in Fig. 3 illustrates that it is difficult for the actuator to generate active force in the bracing at the three natural frequencies of the building, i.e., the structural pole becomes actuator zero. A similar conclusion has been reported for two scaled models presented in [Dyke et al. (1994a, b)]. Therefore, the system identification procedure taking into account the CSI effect was conducted in the following where the resulting analytical system equation is continuous in time and discrete in space.

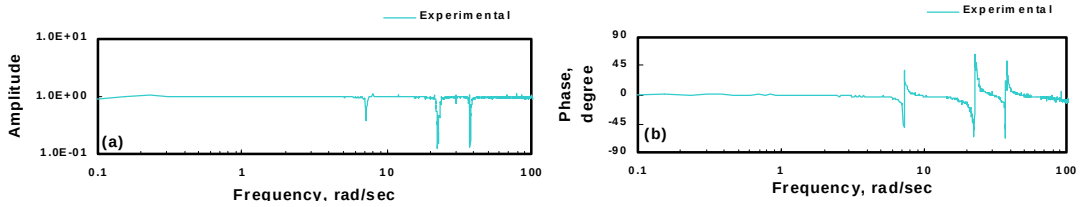

Fig. 3: Transfer Function of Actuator Installed in the Building; (a) Amplitude, and (b) Phase Angle

Since the actively controlled building has two input sources, i. e., the earthquake excitation and the actuator command, it is expediently assumed that the total responses of the eight recorded quantities in **z** are the superposition of those induced by each individual input source. The validity of this assumption will be verified by the experimental results later. With the input of a 0-10 Hz banded white noise earthquake excitation, the transfer functions of eight recorded response quantities are computed using the FFT technique. For instance, the transfer functions of x_3 and $\ddot{x}_{1a}$ are shown in Fig. 4 by dotted curves. Then, each transfer function can be curve-fitted by a rational ratio of two polynomials, $(b_n s^n + b_{n-1}s^{n-1} + ... + b_1 s + b_0)/(s^m + a_{m-1}s^{m-1} + ... + a_1 s + a_0)$, in the Laplace domain, where s is the Laplace variable. The coefficients $b_n, b_{n-1}, ..., b_1, b_0, a_{m-1}, ..., a_1, a_0$ can be determined by a weighted least-square-error method, leading to the solution of a set of simultaneous algebraic equations given by

$$real\begin{bmatrix} \mathbf{\Omega}^*\mathbf{\Lambda}\mathbf{\Omega} & \mathbf{\Omega}^*\mathbf{\Lambda}\mathbf{\Gamma} \\ -\mathbf{\Gamma}^*\mathbf{\Lambda}\mathbf{\Omega} & \mathbf{\Gamma}^*\mathbf{\Lambda}\mathbf{\Gamma} \end{bmatrix}\begin{bmatrix} \{\mathbf{b}\} \\ \{\mathbf{a}\} \end{bmatrix} = real\begin{bmatrix} \mathbf{\Omega}^*\mathbf{\Lambda}\mathbf{F} \\ -\mathbf{\Gamma}^*\mathbf{\Lambda}\mathbf{F} \end{bmatrix} \tag{1}$$

in which

$$\mathbf{\Omega} = \begin{bmatrix} (iw_1)^n & \cdots & (iw_1) & 1 \\ (iw_2)^n & \cdots & (iw_2) & 1 \\ \vdots & \cdots & \vdots & \vdots \\ (iw_N)^n & \cdots & (iw_N) & 1 \end{bmatrix}; \mathbf{\Gamma} = \begin{bmatrix} (iw_1)^{m-1} g_1 & (iw_1)^{m-2} g_1 & \cdots & (iw_1) g_1 \\ (iw_2)^{m-1} g_2 & (iw_2)^{m-2} g_2 & \cdots & (iw_2) g_2 \\ \vdots & \vdots & \cdots & \vdots \\ (iw_N)^{m-1} g_N & (iw_N)^{m-2} g_N & \cdots & (iw_N) g_N \end{bmatrix} \tag{2}$$

$$\mathbf{\Lambda} = diag(\lambda_1, \lambda_2, ..., \lambda_N);\ \mathbf{F} = \begin{bmatrix} (iw_1)^m g_1 \\ (iw_2)^m g_2 \\ \vdots \\ (iw_N)^m g_N \end{bmatrix};\ \{\mathbf{a}\} = \begin{bmatrix} a_{m-1} \\ \vdots \\ a_1 \\ a_0 \end{bmatrix};\ \{\mathbf{b}\} = \begin{bmatrix} b_n \\ \vdots \\ b_1 \\ b_0 \end{bmatrix}$$

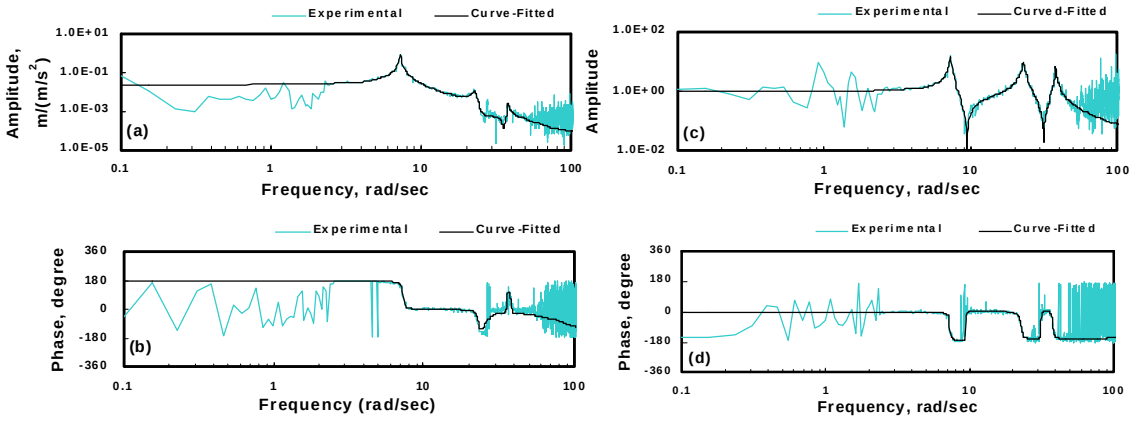

Fig. 4: Transfer Functions of the Building due to White Noise Earthquake; (a) Amplitude of x_3 , (b) Phase Angle of x_3 , (c) Amplitude of $\ddot{x}_{1a}$, and (d) Phase Angle of $\ddot{x}_{1a}$

In Eq. (1), the superscript * represents complex conjugate and transpose. In Eq. (2), $i = \sqrt{-1}$; g_j is the value of the jth data point in the recorded transfer function corresponding to the frequency w_j ; N is the total number of data points in the recorded transfer function; and λ_j is the adjustable weighting parameter for the jth data point in the least-square-error method. We use 6th order polynomials (i.e., m=n=6) for the denominator and numerator of each transfer function. Further, in order to maintain the same denominator for such a single-input-multiple-output case, Eqs. (1) and (2) are first used for curve-fitting the transfer function of the recorded 3rd floor absolute acceleration to compute the coefficients $b_n, b_{n-1}, ..., b_1, b_0, a_{m-1}, ..., a_1, a_0$. Then, the resulting coefficients $a_{m-1}, ..., a_1, a_0$ (common denominator polynomial) are used for curve-fitting other recorded transfer functions to obtain their individual $b_n, b_{n-1}, ..., b_1, b_0$ by solving the upper equation in Eq. (1). Due to space limitation, only the curve-fitted plots of x_3 and $\ddot{x}_{1a}$ are shown in Fig. 4 , denoted by the solid curves, for demonstrative purpose. Consequently, the eight transfer functions can be converted into a set of state-space equations in the time domain expressed by

$$\dot{\mathbf{Z}}_1 = \mathbf{A}_1\mathbf{Z}_1 + \mathbf{B}_1\mathbf{W}; \qquad \mathbf{z}_1 = \mathbf{C}_1\mathbf{Z}_1 + \mathbf{D}_1\mathbf{W} \tag{3}$$

in which $\mathbf{Z}_1$ is a state vector; $\mathbf{W}$ is the earthquake acceleration; $\mathbf{z}_1$ is a vector containing the eight recorded quantities; and $\mathbf{A}_1$, $\mathbf{B}_1$, $\mathbf{C}_1$, $\mathbf{D}_1$ are constant matrices with appropriate dimensions. In Eq. (3), the eigenvalues of $\mathbf{A}_1$ are found to be –0.110±7.275i, -0.545±22.846i and –0.468±37.939i where the real and imaginary parts represent the damping effect and frequency, respectively. It is observed that these three frequencies are close to what is obtained in the preliminary study. Since the transfer functions are curve-fitted well, the response time histories obtained from numerical simulations using Eqs. (3) under the excitation of 0.1g El Centro and Kobe earthquakes correlate remarkably well with the experimental results as expected.

In the same manner, the transfer functions of eight recorded response time histories can be computed when a 0-30 Hz banded white noise of actuator command is used as the input (e. g., see Fig. 5 for x_3 and $\ddot{x}_{1a}$). For this situation, two cases are considered for curve-fitting, first for $\ddot{x}_{1a}$, $\ddot{x}_{2a}$, $\ddot{x}_{3a}$ and second for x_1, x_2, x_3, x_f and f . In the first case, since the accelerations $\ddot{x}_{1a}$, $\ddot{x}_{2a}$, $\ddot{x}_{3a}$ contain more high frequency components, a 12th order polynomial (m=n=12) is used for the denominators and numerators of the transfer functions of $\ddot{x}_{1a}$, $\ddot{x}_{2a}$, $\ddot{x}_{3a}$. In this case, the common denominator is obtained from the 3rd floor absolute acceleration $\ddot{x}_{3a}$. The curve-fitted results of $\ddot{x}_{1a}$ is shown in Figs. 5 (c) and (d). The three curve-fitted transfer functions are converted into a state-space equation given by

$$\dot{\mathbf{Z}}_2 = \mathbf{A}_2\mathbf{Z}_2 + \mathbf{B}_2\mathbf{U}; \quad \mathbf{z}_2 = \mathbf{C}_2\mathbf{Z}_2 + \mathbf{D}_2\mathbf{U} \tag{4}$$

In Eq. (4), $\mathbf{Z}_2$ is a state vector; $\mathbf{U}$ is the actuator command; $\mathbf{A}_2$, $\mathbf{B}_2$, $\mathbf{C}_2$ and $\mathbf{D}_2$ are constant matrices; and $\mathbf{z}_2$ is a vector containing the same eight quantities as in $\mathbf{z}$, where the coefficients in $\mathbf{C}_2$ and $\mathbf{D}_2$ for x_1, x_2, x_3, x_f, f are zeros. $\mathbf{A}_2$ has 12 eigenvalues as follows: -0.111±7.254i, -0.481±23.316i, -0.448±37.896i, -0.696±56.549i, -0.532±105.277i and –8.263±134.815i. It is observed that $\mathbf{A}_2$ not only contains 6 eigenvalues that are very close to those of $\mathbf{A}_1$ representing the building dynamics, but also contains 6 additional eigenvalues that come from the dynamics of control devices and the CSI effect. Therefore, the control-structure interaction is implicitly involved in Eq. (4). Likewise, the response time histories obtained from numerical simulations using Eq. (4), under the same input of white noise actuator command, correlate well with the experimental results..

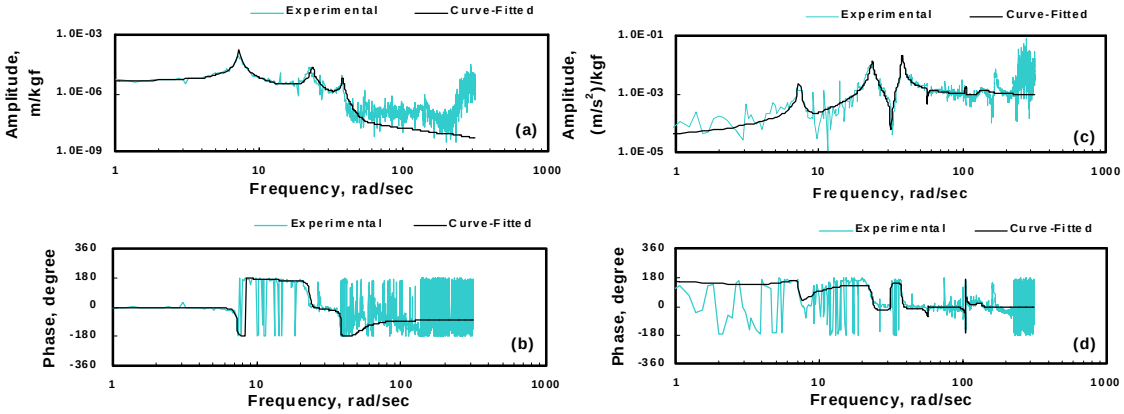

Fig. 5: Transfer Functions of the Building due to White Noise Actuator Command;
(a) Amplitude of x_3, (b) Phase Angle of x_3, (c) Amplitude of $\ddot{x}_{1a}$, and
(d) Phase Angle of $\ddot{x}_{1a}$

In the second case, since the transfer functions of x_1, x_2, x_3, x_f and f have only three peaks (three poles), the first three pairs of the eigenvalues of $\mathbf{A}_2$ is used to construct the common polynomial denominator (m=6) for curve-fitting the transfer functions of x_1, x_2, x_3, x_f and f with n=6. The results of curve-fitting for x_3 are shown in Figs. 5 (a) and 5 (b). The resulting state-space equation is given by

$$\dot{\mathbf{Z}}_3 = \mathbf{A}_3\mathbf{Z}_3 + \mathbf{B}_3\mathbf{U}, \qquad \mathbf{z}_3 = \mathbf{C}_3\mathbf{Z}_3 + \mathbf{D}_3\mathbf{U} \tag{5}$$

In Eq. (5), $\mathbf{Z}_3$ is a state vector; $\mathbf{A}_3$, $\mathbf{B}_3$, $\mathbf{C}_3$ and $\mathbf{D}_3$ are constant matrices; $\mathbf{z}_3$ is a vector containing the same eight quantities as in $\mathbf{z}$, where the coefficients in $\mathbf{C}_3$ and $\mathbf{D}_3$ for $\ddot{x}_{1a}$, $\ddot{x}_{2a}$, $\ddot{x}_{3a}$ are zeros. Again, the response time histories obtained using Eq. (5) for x_1, x_2, x_3, x_f and f, under the same input of white noise actuator command, correlate well with the experimental results.

With the presence of both input sources (earthquake and actuator command), the recorded response vector $\mathbf{z}$ can be obtained by the superposition of $\mathbf{z}_1$, $\mathbf{z}_2$ and $\mathbf{z}_3$, i.e.,

$$\mathbf{z} = \mathbf{C}_\mathbf{z}\mathbf{Z} + \mathbf{D}_\mathbf{z}\mathbf{U} + \mathbf{F}_\mathbf{z}\mathbf{W}\ ;\ \mathbf{C}_\mathbf{z} = \begin{bmatrix}\mathbf{C}_1 & \mathbf{C}_2 & \mathbf{C}_3\end{bmatrix}\ ;\ \mathbf{D}_\mathbf{z} = \mathbf{D}_2 + \mathbf{D}_3\ ;\ \mathbf{F}_\mathbf{z} = \mathbf{D}_1 \tag{6}$$

and the overall state equation can be expressed by

$$\dot{\mathbf{Z}} = \mathbf{A}\mathbf{Z} + \mathbf{B}\mathbf{U} + \mathbf{E}\mathbf{W}\ ;\ \mathbf{Z} = \begin{bmatrix}\mathbf{Z}_1\\ \mathbf{Z}_2\\ \mathbf{Z}_3\end{bmatrix};\ \mathbf{A} = \begin{bmatrix}\mathbf{A}_1 & 0 & 0\\ 0 & \mathbf{A}_2 & 0\\ 0 & 0 & \mathbf{A}_3\end{bmatrix};\ \mathbf{B} = \begin{bmatrix}0\\ \mathbf{B}_2\\ \mathbf{B}_3\end{bmatrix};\ \mathbf{E} = \begin{bmatrix}\mathbf{B}_1\\ 0\\ 0\end{bmatrix} \tag{7}$$

Since the CSI effect in this full-scale building is significant as previously mentioned, it is desirable to design the active controllers based on Eqs. (6) and (7) that include the effect of control-structure interaction. In designing

the active controller, **z** in Eq. (6) can be used as the controlled output for the control objective, whereas the measured output **y,** that is used as the feedback quantities, can be constructed from **z** and expressed as

$$\mathbf{y} = \mathbf{C_y Z} + \mathbf{D_y U} + \mathbf{F_y W} \tag{8}$$

System Reduction for Controllability and Observability

To ensure the controllability and observability, a minimal realization to be used as the nominal system should be constructed for controller design. A well-known system reduction technique, referred to as the balanced state reduction method [Moore 1981], is used herein. An 8-dimensional reduced-order system to be used as the nominal system is obtained as

$$\dot{\mathbf{Z}}_\mathbf{r} = \mathbf{A_r Z_r} + \mathbf{B_r U} + \mathbf{E_r W}; \qquad \mathbf{z_r} = \mathbf{C_{zr} Z_r} + \mathbf{D_{zr} U} + \mathbf{F_{zr} W} \tag{9}$$

The measured output in the reduced-order system can be constructed from the control output $\mathbf{z_r}$ and written as

$$\mathbf{y_r} = \mathbf{C_{yr} Z_r} + \mathbf{D_{yr} U} + \mathbf{F_{yr} W} + \mathbf{v} \tag{10}$$

in which **v** is the measurement-induced noise.

LQG CONTROL STRATEGY

To demonstrate the accuracy of the analytical model constructed above for predicting the controlled building response, 5 sets of controllers have been designed based on the nominal system, Eqs. (9)-(10), using the Linear Quadratic Gaussian (LQG) method. These LQG controllers were used in the shake table experimental tests for the full-scale building. The LQG controller is derived based on the assumption that the excitation **W** and the measurement noise **v** are uncorrelated Gaussian white noise processes. The control objective is to minimize a quadratic objective function

$$J = \lim_{\tau\to\infty} \frac{1}{\tau} \mathbf{E} \left\{ \int_0^\tau (\bar{\mathbf{z}}' \mathbf{Q} \bar{\mathbf{z}} + \mathbf{U}' \mathbf{R} \mathbf{U}) \, dt \right\} \tag{11}$$

in which $\bar{\mathbf{z}} = \mathbf{z_r} - \mathbf{F_{zr} W} = \mathbf{C_{zr}\ Z_r} + \mathbf{D_{zr}\ U}$ (see Eq. (9)), and **Q** and **R** are weighting matrices. Due to space limitation, the detailed derivation is referred to [Skelton (1988), Wu et al (1998b)]. For the on-line computation of the control command **U**, the dynamic output feedback equation is obtained as follows

$$\dot{\mathbf{q}} = \mathbf{A_c\ q} + \mathbf{B_c\ y}; \qquad \mathbf{U} = \mathbf{C_c\ q} + \mathbf{D_c\ y} \tag{12}$$

in which **q** is a state vector to be computed on-line in real time from the measured output **y**, and $\mathbf{A_c}, \mathbf{B_c}, \mathbf{C_c}, \mathbf{D_c}$ are constant matrices obtained from the LQG design. For control implementations, the dynamic output feedback controller, Eq.(12), is further discretized into a discrete form using a sampling rate of 0.002 sec, i.e.,

$$\mathbf{q}(n+1) = \mathbf{A_d\ q}(n) + \mathbf{B_d\ y}(n); \qquad \mathbf{U}(n) = \mathbf{C_d\ q}(n) + \mathbf{D_d\ y}(n) \tag{13}$$

CORRELATION BETWEEN EXPERIMENTAL AND SIMULATION RESULTS

Five sets of LQG controllers, denoted by LQG1, LQG2, LQG3, LQG4 and LQG5, are designed and implemented on the full-scale building for the shake table experimental tests. The first three controllers measure $\ddot{x}_{1a}$, $\ddot{x}_{2a}$, $\ddot{x}_{3a}$ as the feedback quantities, whereas the last two measure $\ddot{x}_{1a}$ only. The earthquakes used are the 1940 El Centro (100 seconds) and 1995 Kobe (60 seconds) earthquakes with a PGA of 0.1g. To verify the accuracy of the analytical model constructed above for predicting the controlled response, numerical simulations using the analytical model, Eqs. (6)-(8), are conducted, and the simulation results are compared with those of the shake table experimental tests. Due to space limitation, only the correlation results under 0.1g El Centro earthquake for the LQG3 controller (larger control command) are presented in Fig. 6 and Table 1. The correlation results for other controllers are similar. As observed from Fig. 6, the correlations between the simulated response time histories and the experimental results are quite remarkable. Table 1 presents the peak and rms values of the building response quantities, the actuator stroke x_f, the active bracing force f and the

actuator command U. It is observed from Table 1 that the correlations between the experimental and simulation results are quite remarkable for the building response quantities as well as the actuator stroke x_f, the active bracing force *f* and the actuator command U.

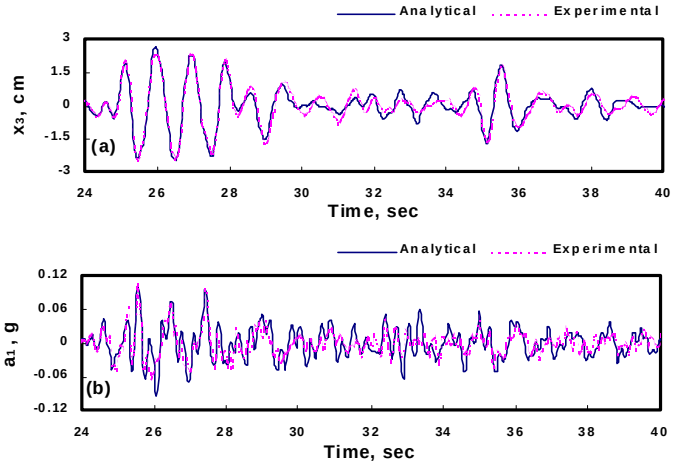

Fig. 6: Correlations of Experimental and Simulated Response Time Histories of the Building under 0.1g El Centro Earthquake Using LQG3 Controller; (a) x_3, and (b) $\ddot{x}_{1a}$

Table 1 : Comparisons of Experimental and Simulated Responses of the Building under 0.1g El Centro Earthquake Using LQG3 Controller

	Experiment		Simulation	
	peak	rms	peak	rms
x_1 (cm)	1.104	0.159	1.339	0.166
x_2 (cm)	1.969	0.292	2.239	0.319
x_3 (cm)	2.488	0.371	2.652	0.384
x_f (cm)	0.885	0.127	1.167	0.154
$\ddot{x}_{1a}$ (g)	0.106	0.010	0.101	0.013
$\ddot{x}_{2a}$ (g)	0.127	0.014	0.133	0.017
$\ddot{x}_{3a}$ (g)	0.196	0.019	0.170	0.021
f (kgf)	1556	195.3	1725	221.0
U (kgf)	1457	185.8	1657	205.8

CONCLUSIONS

Shake table experimental tests using a 3-story full-scale building equipped with active bracing systems have been conducted in this paper. Experimental results show that the control-structure interaction (CSI) effect is significant for the design of dynamic output controllers. A state-space analytical model of the actively controlled building taking into account the CSI effect has been constructed using a system identification technique that is based on the curve-fitting of transfer functions. To verify the accuracy of the analytical model for simulating the controlled response, five LQG controllers using acceleration feedbacks have been implemented on the full-scale building and further shake table tests have been conducted. It is demonstrated that the correlations between the simulation and experimental results are remarkable. The state-space analytical model established herein provides opportunities for future benchmark studies of different control algorithms. The information of the analytical model presented is available on the web site URL: www.ce.tku.edu.tw/~jcwu/research/earth.html.

ACKNOWLEDGMENT

This research is supported by the National Science Council of Taiwan through Grant No. NSC88-2211-E032-002. Valuable discussion and advices from Dr. L. L. Chung, Dr. L. Y. Lu and laboratory manager C. P. Cheng of NCREE are gratefully acknowledged.

REFERENCES

Chung, L. L., Lin, R. C., Soong, T. T. and Reinhorn, A. M. (1989), "Experiments on Active Control for MDOF Seismic Structures", *ASCE Journal of Engineering Mechanics*, Vol. 115, No. 8, pp. 1609-1627.

Chung, L. L., Lin, C. C. and Lu, K. H. (1995), "Time Delay Control of Structures", Earthquake Engineering and Structural Dynamics, Vol. 24, pp. 687-701.

Dyke, S. J., Spencer, B. F., Belknap, A. E., Ferrell, K. J., Quast, P. and Sain, M. K.(1994a), "Absolute Acceleration Feedback Control Strategies for the Active Mass Driver", *Proceedings of 1st World Conference on Structural Control*, Vol. 2, pp. TP1-51~TP1-60.

Dyke, S. J., Spencer, B. F., Quast, P., Sain, M. K., Kaspari, D. C. and Soong, T. T. (1994b), "Experimental Verification of Acceleration Feedback Control Strategies for an Active Tendon System", *National Center for Earthquake Engineering Research Technical Report*, NCEER-94-0024.

Dyke, S. J., Spencer, B. F., Quast, P., and Sain, M. K. (1994c), "The Role of Control-Structure Interaction in Protective System Design", *ASCE Journal of Engineering Mechanics*,

Kobori, T., Inoue, Y., Seto, K., Iemura, H. and Nishitani, A. (editors) (1998), *Proceedings of Second World Conference on Structural Control*, John Wiley & Sons, N. Y.

Moore, B. C. (1981), "Principal Component Analysis in Linear System: Controllability, Observability and Model Reduction", *IEEE Transactions on Automatic Control*, Vol. 26, No. 1, pp. 17-32.

Skelton, R. E. (1988), *Dynamic Systems Control : Linear Systems Analysis and Synthesis*, John Wiley, NY.

Spencer, B. F., Suhardjo, J., and Sain, M. K. (1994), "Frequency Domain Optimal Control Strategies for Seismic Protection", *ASCE Journal of Engineering Mechanics*, Vol. 120, No. 1, pp. 135-156.

Wu, J. C., Yang, J. N. and Schmitendorf, W., (1998a), "Reduced-Order H_∞ and LQR Control for Wind-Excited Tall Buildings", *Journal of Engineering Structures*, Vol. 20, No. 3, pp. 222-236.

Wu, J. C. and Yang, J. N., (1998b), "Active Control of Transmission Tower under Stochastic Wind", *ASCE Journal of Structural Engineering*, Vol. 124, No. 11, pp. 1302-1312.

Yang, J. N. (1975), "Application of Optimal Control Theory to Civil Engineering Structures", *ASCE Journal of Engineering Mechanics Division*, Vol. 101, No. EM6, pp. 819-838.

Yang, J. N., Wu, J. C and Agrawal, A. K. (1995), "Sliding Mode Control of seismically excited linear structures", *Journal of Engineering Mechanics*, Vol. 121, No. 12, pp. 1386-1390.

Yang, J. N., Wu, J. C., Reinhorn, A. M., Riley, M., Schmitendorf, W. E.and Jabbari, F. (1996a), "Experimental Verification of H Infinity and Sliding Mode Control for Seismic-Excited Buildings", *ASCE Journal of Structural Engineering*, Vol. 122, No. 1, pp. 69-75.

Yang, J. N., Wu, J. C., Reinhorn, A. M. and Riley, M. (1996b), "Control of Sliding-Isolated Buildings Using Sliding Mode Control", *ASCE Journal of Structural Engineering*, Vol. 122, No. 2, pp. 179-186.

Yang, J. N., Wu, J. C, Agrawal, A. K. and Hsu, S. Y. (1997), "Sliding Mode Control with Compensators for Wind and Seismic Response Control", *Journal of Earthquake Engineering and Structural Dynamics*, Vol. 26, pp. 1137-1156.